Tellus (2004), 56A, 102–111
Printed in UK. All rights reserved

TELLUS

Numerical simulations of Greenland's impact on the Northern Hemisphere winter circulation

By GUÐRÚN NÍNA PETERSEN[1,2,*], JÓN EGILL KRISTJÁNSSON[1] and HARALDUR ÓLAFSSON[2,3], [1]*Department of Geosciences, University of Oslo, Pb 1022 Blindern, 0315 Oslo, Norway;* [2]*University of Iceland, Iceland;* [3]*Icelandic Meteorological Office and Institute for Meteorological Research, Iceland*

(Manuscript received 16 October 2003)

ABSTRACT

The impact of Greenland's orography on the general circulation is investigated. Two 10-yr simulations are conducted using the National Center for Atmospheric Research (NCAR) Community Climate Model (CCM3) at T106 horizontal resolution (spectral truncation): a control simulation and a simulation where Greenland's orography is set to sea level. A comparison of the simulations indicates that Greenland has a significant impact on the general circulation of the Northern Hemisphere at both lower and mid-tropospheric levels. The storm tracks over the North Atlantic are shifted southward in the presence of the mountain. There are significant differences between the two simulations over a large area in the Northern Hemisphere. It is argued that this difference pattern is linked to the damming of cold low-level air masses west of Greenland that result in a decrease in the 500-hPa geopotential height on the upstream side of the mountain. Thus, Greenland's impact on the general circulation is fundamentally different from the impact of the Rocky Mountains and the Tibetan Plateau where westerlies impinging on a major mountain range create a trough downstream of the mountain.

1. Introduction

Greenland is one of the largest mountains in the Northern Hemisphere with a maximum height of bedrock and ice cap exceeding 3500 m and a total area of over two million km^2. It is located much farther north than the two large mountain ranges, the Rocky Mountains and the Tibetan Plateau, with its southern tip at about 60°N and a northward extension of 2500 km. Greenland's location is close to the North Atlantic storm tracks and cyclones move northward along both its southeastern and southwestern coast. The upper-level polar vortex is in the mean located in the vicinity of Greenland while there are strong westerlies at middle tropospheric levels near the other mountain ranges mentioned. Furthermore, during winter there are large horizontal temperature gradients in its vicinity. To the west there are cold land masses and sea ice while the relatively warm North Atlantic is to the south and east of Greenland. However, despite its size and location, little is known about its impact on the general circulation.

The meteorological research on the effect of Greenland has mainly been limited to the atmosphere in the immediate vicinity of Greenland itself. Extensive work has been done studying the surface energy balance, precipitation and snow accumulation (e.g. Chen et al., 1997; McConnel et al., 2000; Denby et al., 2002). Furthermore, katabatic flow over Greenland has been studied in field experiments (e.g. KABEG'97) and by numerical simulations (e.g Bromwich et al., 1996; Heinemann, 1999; Bromwich et al., 2001; Klein et al., 2001; Heinemann and Klein, 2002a,b). On a slightly larger scale, the impact of Greenland as a large mountain has gained some attention through case studies. They have mainly focused on Greenland's impact on the airflow east of southern Greenland and found Greenland's orography to be important for the synoptic systems in its vicinity (e.g. Ólafsson, 1998; Doyle and Shapiro, 1999; Kristjánsson and McInnes, 1999). Petersen et al. (2003) studied flow in the vicinity of idealized mountains and Greenland. They found that a large mountain can increase the geopotential gradient aloft south of the mountain wake and thus influence the airflow far from the mountain. This can result in a positive impact on both depth and propagation speed of cyclones moving far south of the mountain. Schwierz (2001) studied the interaction of Greenland-scale orography and extratropical synoptic-scale flow. She noticed that Greenland-scale orography impacts the atmosphere in a large variety of ways, e.g. the cyclones within the storm tracks can experience large horizontal deflections. The studies mentioned above indicate the possibility that Greenland not only affects the atmospheric flow in its vicinity but also in areas farther downstream.

*Corresponding author.
e-mail: g.n.petersen@geo.uio.no

To the southeast of southern Greenland, there is a climatological minimum in the mean sea level pressure, often referred to as the Icelandic low. Held (1983) showed that the Icelandic low owed its existence at least partly to thermal forcing. However, the model resolution in his study was coarse and Greenland was poorly described. Consequently, the effect of Greenland on the climatological Icelandic low remained unclear.

The purpose of this study is to seek answers to the following question. How does Greenland affect the Northern Hemispheric circulation on large spatial and temporal scales? To address the question, two simulations are conducted with a fine-resolution general circulation model (GCM), a control simulation and a simulation where Greenland's orography is removed. They are compared and discussed, and compared to observations.

The following section includes a short description of the model and the data used. The results are described in Section 3, a discussion is given in Section 4 and finally summary and conclusions appear in Section 5.

2. The experimental set-up

2.1. The model set-up

The National Center for Atmospheric Research (NCAR) Community Climate Model (CCM3) is applied in this study (Kiehl et al., 1998). The CCM3 is a stable, efficient and well-documented state-of-the-art atmospheric GCM designed for climate research. The standard horizontal resolution that is documented is T42 spectral truncation (approximately $2.8^\circ \times 2.8^\circ$ transform grid). In the present study, in order to resolve Greenland better, T106 spectral resolution (approximately $1.1^\circ \times 1.1^\circ$ transform grid) is applied. Figure 1 shows the actual orography of Greenland as well as the orography at this resolution. The vertical coordinate is a hybrid sigma-pressure coordinate and there are 18 levels. The model time-step is 450 s and the model is run for 10 yr. Due to the change in resolution it is necessary to tune the model slightly in order to maintain radiative equilibrium (Williamson et al., 1995). Table 1 shows the parameters that are changed and Table 2 shows the global annual means of selected quantities from simulations with T42 and T106 spectral resolution. The initial data set includes the T42 CCM3.6 Sep1 atmospheric data set, prepared by NCAR. The CCM3 includes a land surface model and has climatological sea surface temperatures that evolve through the seasonal cycle but are repeated each year.[1] The initial data set, as well as the sea surface data set, is interpolated to the T106 resolution. The gravity wave drag is parametrized by standard deviation of the topography. Further information about the model can be found in Kiehl et al. (1996, 1998).

[1]The Shea, Trenberth, Reynold (National Meteorological Center/ Climate Analysis Center) sea surface temperature (SST) data set prepared by NCAR.

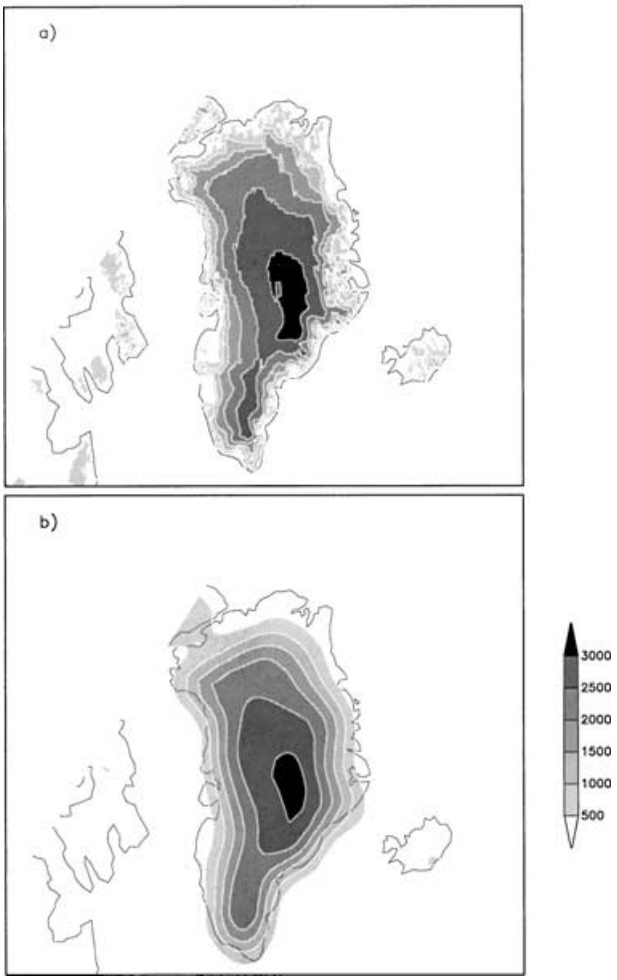

Fig. 1. The height of the topography (m) of Greenland from (a) a high-resolution data set and (b) the CCM3 at T106 spectral resolution. The high-resolution data set is NCAR's data set, based on the US Navy Global Elevation 10-min data set. The contour interval is 500 m.

The experiments consist of two simulations: one control simulation, termed 'CONTROL', and a simulation where the orography of Greenland is set to sea level, termed 'NOGREEN'. The surface characteristics are unchanged, thus the surface is still defined as a glacier. The time it takes to damp the noise due the the removal of Greenland is on the scale of days but the first 15 months of the simulations are regarded as spin-up. The outputs from the model are 10 yr of monthly averaged values, as well as 6-hourly values of a few basic variables including geopotential height and sea level pressure.

The results presented are mean winter (December–February) Northern Hemisphere simulated climates. In order to validate the simulations, the CONTROL simulation is compared to NCEP global reanalysis (Kalnay et al., 1996) climatology (1968–1996). The two simulations CONTROL and NOGREEN are compared by subtracting the results from the NOGREEN simulation from

Table 1. *Parameters changed to tune the model to T106 resolution*

Parameter	T42	T106
Horizontal fourth-order diffusion coefficient ($m^4\ s^{-1}$)	1×10^{16}	1×10^{15}
High and middle cloud relative humidity threshold (%)	0.90	0.80
Low cloud relative humidity threshold (%)	0.90	0.91
Time-step (s)	1200	450
Convective time-scale (s)	3600	1200

Table 2. *Global annual averages of selected quantities from simulations at T42 and T106 spectral resolution*

Quantity	Observation	T42	T106
Total cloud cover (%)	67.6[a)]	0.60	0.58
Low clouds (%)	27.5[a)]	0.35	0.32
Middle clouds (%)	19.0[a)]	0.21	0.21
High clouds (%)	19.6[a)]	0.35	0.34
Convective precipitation (mm d^{-1})		2.61	2.65
Stable precipitation (mm d^{-1})		0.48	0.56
Total precipitation (mm d^{-1})	2.69[b)]	3.09	3.22
Net long-wave radiative flux at the top (W m^{-2})	234.8[c)]	236.0	238.7
Net short-wave radiative flux at the top (W m^{-2})	238.1[c)]	236.3	238.2
Long-wave cloud forcing (W m^{-2})	29.2[c)]	29.5	27.8
Short-wave cloud forcing (W m^{-2})	−48.2[c)]	−50.0	−47.4

[a)]Rossow and Schiffer (1999).
[b)]Xie and Arkin (1996).
[c)]Earth Radiation Budget Experiment (ERBE).

those of the CONTROL simulation. The resulting difference fields present the effect of Greenland. The CCM3 has been shown to simulate the North Atlantic storm track structure quite well at the standard horizontal resolution (Magnusdottir, 2001). In the present study the storm track structure is calculated by band-pass filtering (Blackmon, 1976) the geopotential height of the sigma-pressure level that is approximately at the 500-hPa level.

A t-test is applied to investigate if the differences between the two simulations are significant. The 10 winters in each simulation are assumed independent and all the major differences are found to be at least 95% statistically significant.

2.2. *Validation of the CONTROL simulation*

A comparison between simulated fields and observations gives an indication of the ability of the model to simulate the atmospheric circulation.

The mean sea level pressure pattern indicates how well the model simulates the circulation near the surface and it represents an integrated measure of the model's thermodynamic representation. The mean distribution of sea level pressure in the Northern Hemisphere during winter (DJF) in the control simulation and the NCEP reanalysis as well as the difference field are shown in Fig. 2. Due to the sea level reduction problem, the magnitude of the difference over high terrain is not meaningful. The model reproduces the basic patterns well, the Icelandic and the Aleutian low are captured as well as the subtropical high pressure belt. However, there are some regional biases, known to exist in CCM3, documented for the T42 resolution (Hurrell et al., 1998). During northern winter, the sea level pressure is higher than observed in the subtropics and too low at subpolar latitudes. The Aleutian low does not extend as far east as observed and the high pressure ridge over northern Africa is too strong. The Icelandic low is not closed and erroneously low pressures extend across northern Europe well into Eurasia. Some of these biases seem to be increased by the fine resolution, e.g. the low pressure in subpolar latitudes, especially over the North Atlantic. On the other hand, the errors over the North Pacific and northern Africa are smaller at T106 spectral resolution than at T42. The sea level pressure field in the vicinity of Greenland has much finer structure than at T42 resolution where the high pressure centre over Greenland is not closed and the Icelandic low does not curve around the southern tip of Greenland but simply extends over it (not shown).

The 500-hPa geopotential height field is a representative climate parameter of the mid-tropospheric flow. Figure 3 shows the simulated mean winter 500-hPa geopotential height in the Northern Hemisphere, the NCEP reanalysis and the difference field.

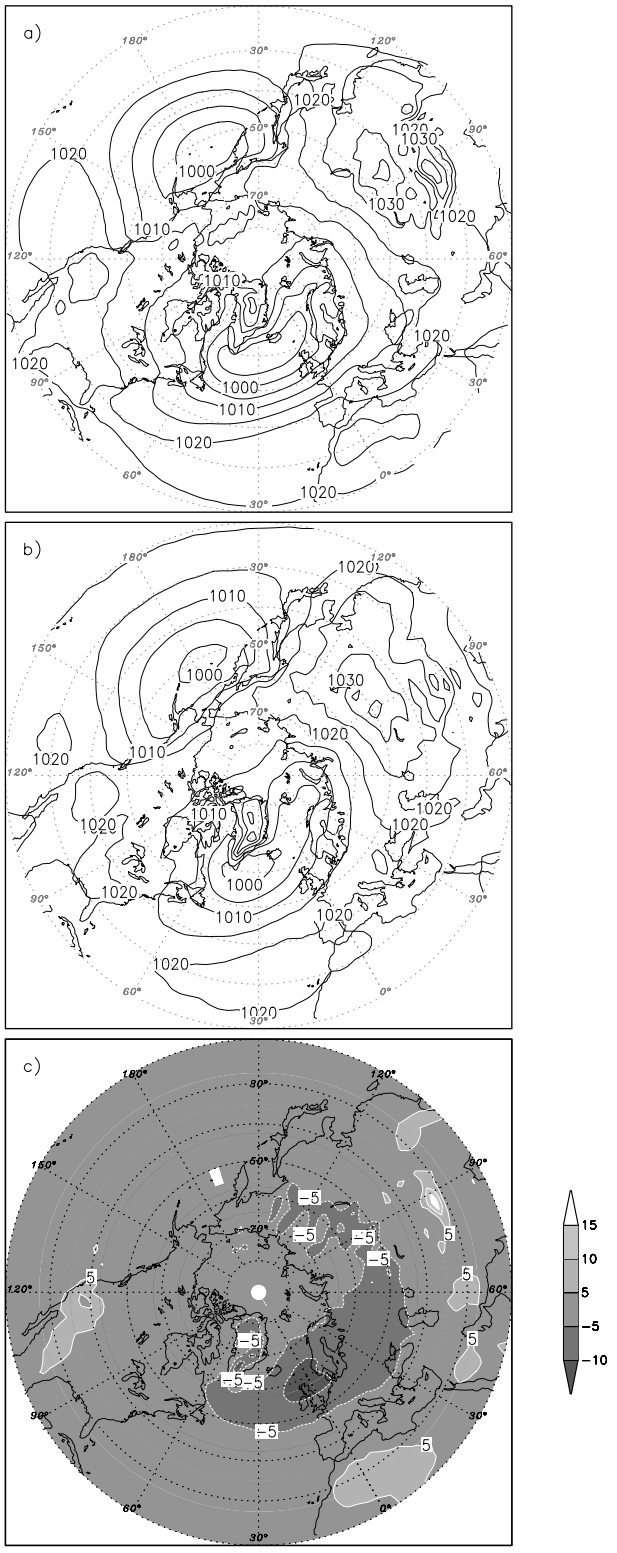

Fig. 2. The mean winter (DJF) sea level pressure (hPa) in (a) the CONTROL simulation, (b) the NCEP reanalysis climatology 1968–1996 and (c) the difference field CONTROL–NCEP. The contour interval is 5 hPa and the zero contour is suppressed in (c).

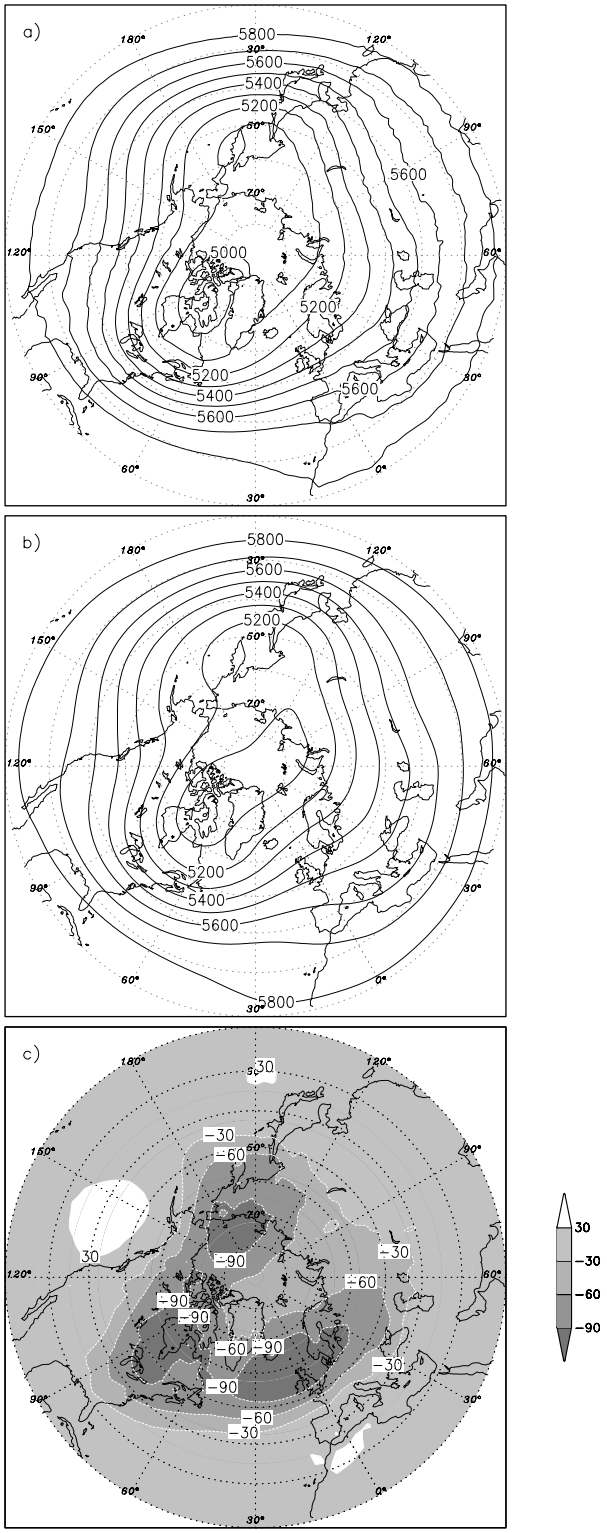

Fig. 3. The mean winter (DJF) 500-hPa geopotential height (gpm) in (a) the CONTROL simulation, (b) the NCEP reanalysis climatology 1968–1996 and (c) the difference field CONTROL–NCEP. The contour interval is 100 gpm in (a) and (b) but 30 gpm in (c) where the zero contour is suppressed.

The major troughs off the east coast of Asia and North America, as well as the trough over eastern Europe, are well reproduced. The ridges over central Asia and the west coast of North America are also well captured. However, the simulated height is lower than observed at high latitudes, which is consistent with a slight cold bias at extratropical latitudes in CCM3 (Hack et al., 1998). Other differences are largely consistent with the sea level pressure errors; for example, the ridge over the west coast of North America is shifted a little to the west of its observed location. The simulated Atlantic ridge is too weak and does not extend as far east as observed. The errors at T106 resolution with respect to T42 resolution are consistent with the sea level pressure errors discussed above. At subpolar latitudes, the biases have increased slightly while they have decreased at mid-latitudes.

The comparison shows that even though there are some regional differences between the CCM3 control simulation and the NCEP reanalysis, the model simulates the atmospheric circulation reasonably well. The CONTROL simulation will therefore in the present study be regarded as an approximation to the atmospheric circulation with Greenland present and the NOGREEN simulation to the circulation when the orography of Greenland has been removed. The difference between the two simulations should give indications of the effect of Greenland's orography on the circulation, assuming that the model biases cancel.

3. Results

Figure 4a shows the mean sea level pressure during the winter in the NOGREEN simulation and Fig. 4b shows the difference field between the two simulations. When Greenland's orography is removed the Icelandic low does not curve around the southern tip of Greenland, as it does in its presence, and the low loses its banana shape. The low is deeper than in the CONTROL simulation and the centre is shifted slightly to the north. The difference field shows that Greenland contributes to higher sea level pressure east and southeast of the mountain while the sea level pressure is lower over southern Europe, Canada and Alaska.

Figure 5a shows the 500-hPa geopotential height in NOGREEN. The trough off the east coast of North America is broader than in the CONTROL simulation with the 500-hPa polar vortex now no longer mainly confined to the west of Greenland but extending farther to the east. The difference field (Fig. 5b) shows that the impact of Greenland is to increase the 500-hPa geopotential height in the Greenland area and over a large part of the North Atlantic, while there is a decrease of the geopotential height to the west of Greenland, centred over Alaska, as well as over southern Europe.

The 1000–500 hPa geopotential thickness can help shed light on the pattern seen in Fig. 5b. Figure 6 shows the mean winter thickness difference between the simulations. Over northern Canada and Alaska as well as over northern Europe the thickness is reduced by Greenland's presence. The thickness over the central part of North America is, on the other hand, significantly increased. Over the North Atlantic east of Greenland, there is little difference between the simulations and the difference is not significant at the 95% level. This will be discussed in more detail in Section 4.

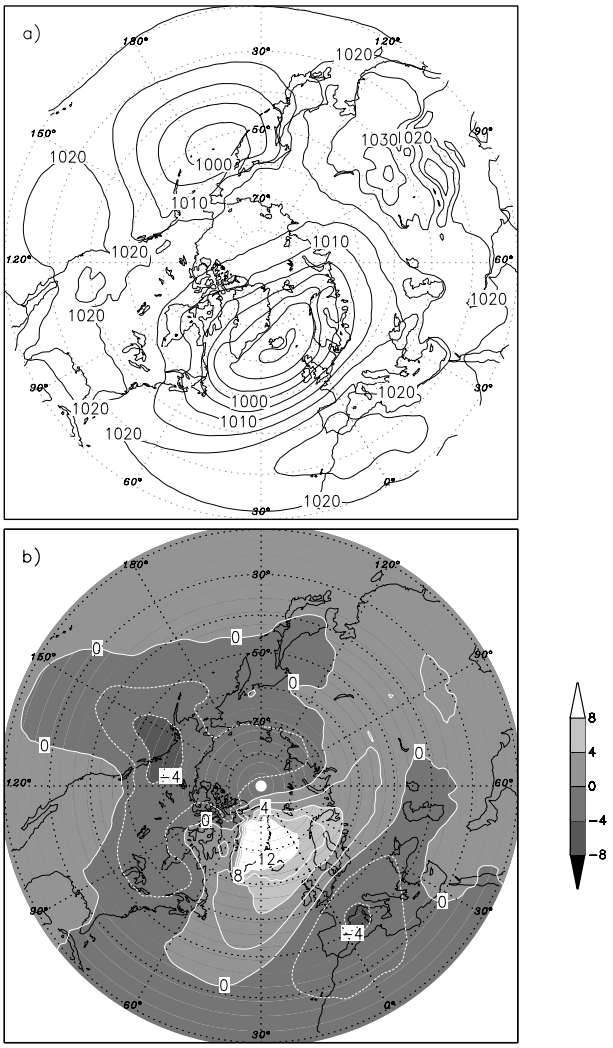

Fig. 4. (a) The mean winter (DJF) sea level pressure (hPa) in the NOGREEN simulation and (b) the mean sea level pressure difference (hPa), CONTROL–NOGREEN. The contour interval is 5 hPa in (a) and 2 hPa in (b). All the major differences in (b) are 95% statistically significant.

Storm tracks can be symbiotically linked to the planetary-scale flow (Chang et al., 2002), that is, there is an intimate relationship between the planetary-scale flow and the storm tracks. It is therefore reasonable to expect some influence on the storm tracks by Greenland's orography. Figure 7a shows the storm track structure at the 500-hPa level in the CONTROL simulation calculated by bandpass filtering the geopotential height data with a 2.5–6 d filter. The storm track structure has its maximum at about 50°N

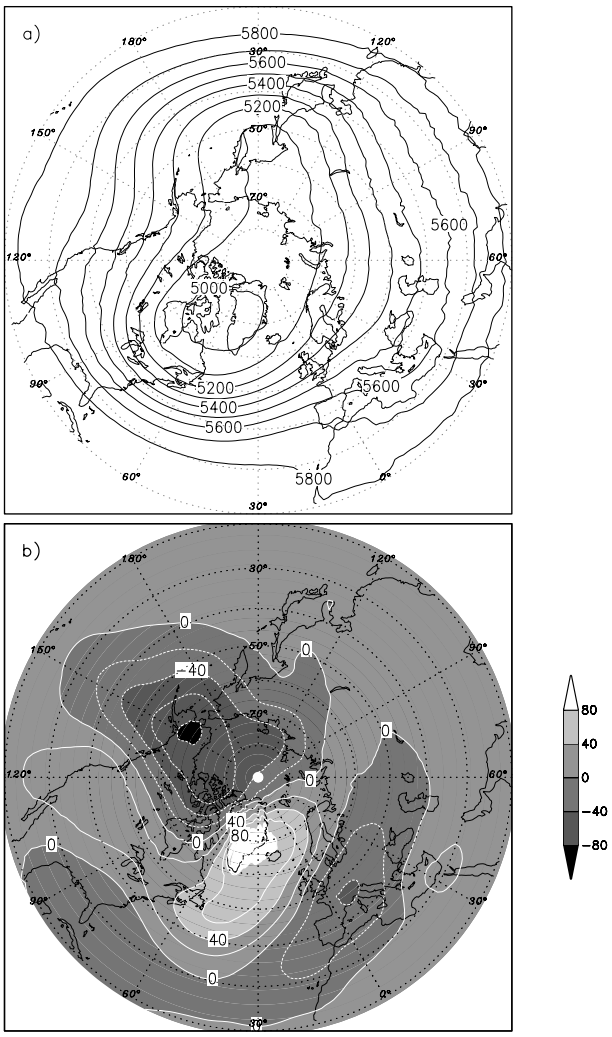

Fig. 5. (a) The mean winter (DJF) 500-hPa geopotential height (gpm) in the NOGREEN simulation and (b) the mean 500-hPa geopotential height difference (gpm), CONTROL–NOGREEN. The contour interval is 100 gpm in (a) and 20 gpm in (b). All the major differences in (b) are 95% statistically significant.

over the North Pacific, North America and the North Atlantic. This maximum is shifted slightly to the south relative to observations (Chang et al., 2002). There is a local maximum in the activity at the southwestern coast of Greenland, the fingerprint of cyclones moving into the Davis Strait. The mountain prevents these cyclones from moving farther east and they therefore follow the western coast of Greenland northward as they decay. Figure 7b shows the difference in extratropical 500-hPa variability between the CONTROL and the NOGREEN simulations. The figure shows Greenland to contributes to more intense storm tracks over North America and the Pacific as well as over northern Asia. Over the North Atlantic and northern Europe the activity is less than in the NOGREEN simulation. The storm track structure will be discussed further in Section 4.

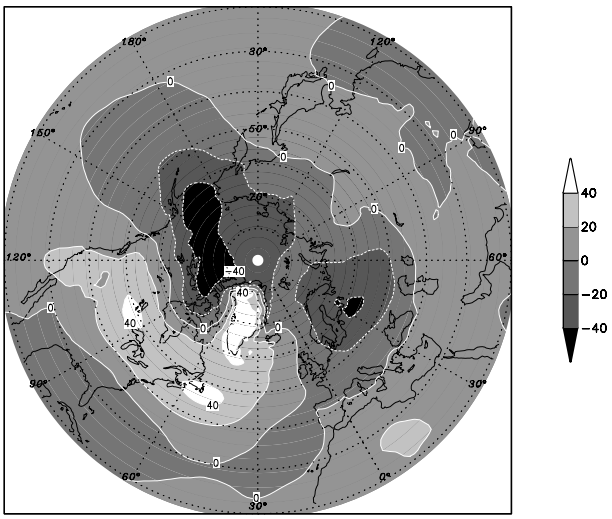

Fig. 6. The mean winter (DJF) 500–1000 hPa thickness (gpm) difference, CONTROL–NOGREEN. The contour interval is 20 gpm and all the major differences are 95% statistically significant.

Figure 8 shows the mean winter precipitation difference. When the Greenland mountain is present, there is considerably more precipitation at the southern tip of Greenland, along its southeastern coast and at the west coast of Canada. At the western coast of Norway there is a 2 mm d^{-1} reduction in the precipitation rate, while the decrease over the North Atlantic is about 1 mm d^{-1}. However, relative to the total precipitation rate in the CONTROL simulation (not shown), only the difference in the Greenland area is large, accounting for more than half of the precipitation rate. Note that the large precipitation values near the southern tip of Greenland in the CONTROL simulation (about 8 mm d^{-1}, not shown) are supported by observations (Putnins, 1970). This maximum in precipitation is probably caused by combined effects of some cyclones moving into the Davis Strait and orographic lifting at the steep slopes of the southeastern coast of Greenland.

The North Atlantic Oscillation (NAO) index is a common measurement of the variation in the strength of the zonally averaged middle latitude surface westerlies and thus a reflection of the variation in the NAO (Hurrell et al., 2003). Figure 9 shows the NAO index in the two simulations calculated for December–February between Stykkishólmur, Iceland (65°N 22°W) and Lisbon, Portugal (38°N 09°W). There is not a clear difference between the simulations. During the first six years, the CONTROL simulation has a larger NAO index than NOGREEN, while it has a lower NAO index for the last four years. An empirical orthogonal function (EOF) analysis of the sea level pressure in the simulations shows the first EOF in both simulations to reflect the Northern Hemispheric Annual Mode (NAM) as can be seen in Fig. 10. The EOF 1 signal at polar latitudes in the CONTROL simulation is shifted to the east relatively to EOF analysis of observed data (fig. 8 in Hurrell et al., 2003). The signal in the

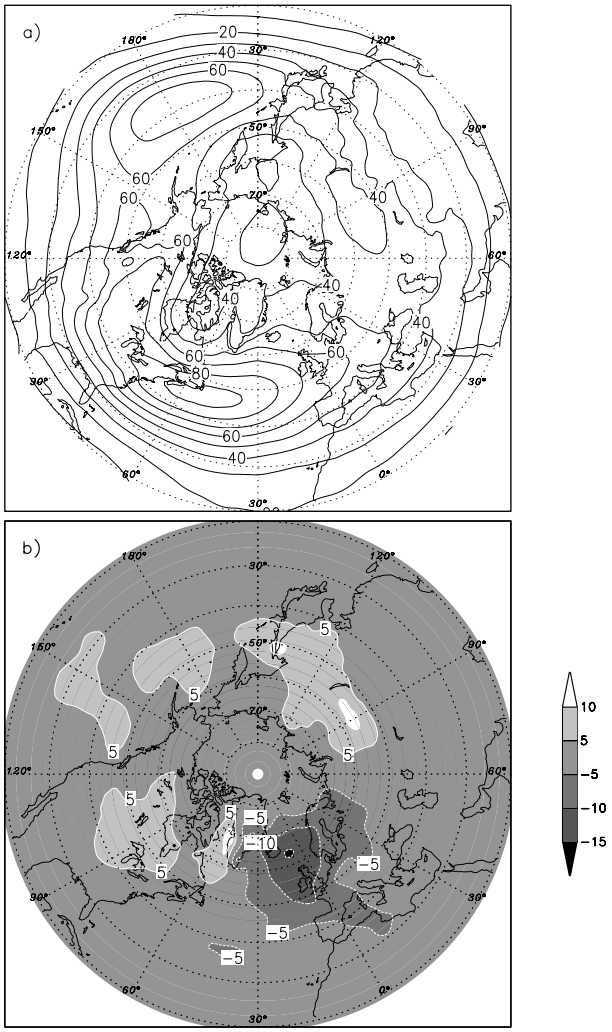

Fig. 7. The winter (DJF) 500-hPa geopotential height 2.5–6 d bandpass statistics. (a) Root mean square standard deviation (gpm) and (b) the difference root mean square standard deviation field, CONTROL–NOGREEN (gpm). The contour interval is 10 gpm in (a) and 5 gpm in (b). The zero contour is suppressed.

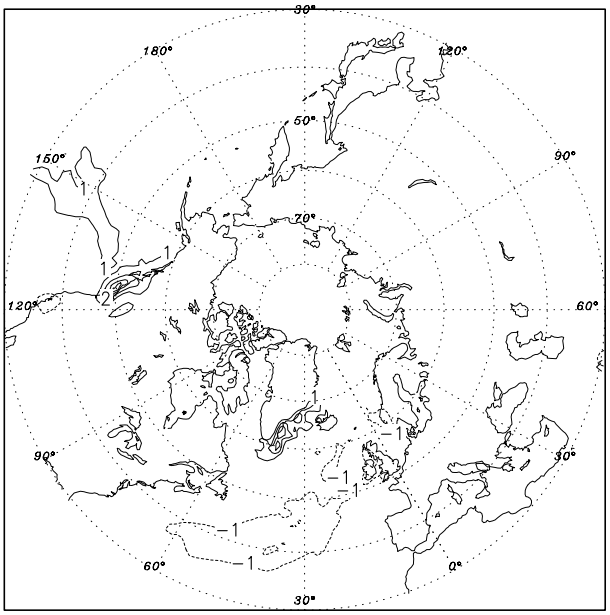

Fig. 8. Difference in mean winter (DJF) precipitation rate CONTROL–NOGREEN. The contours show the difference in mm d^{-1}. The interval is 1 mm d^{-1} and the zero contour is suppressed. The differences are 95% statistically significant.

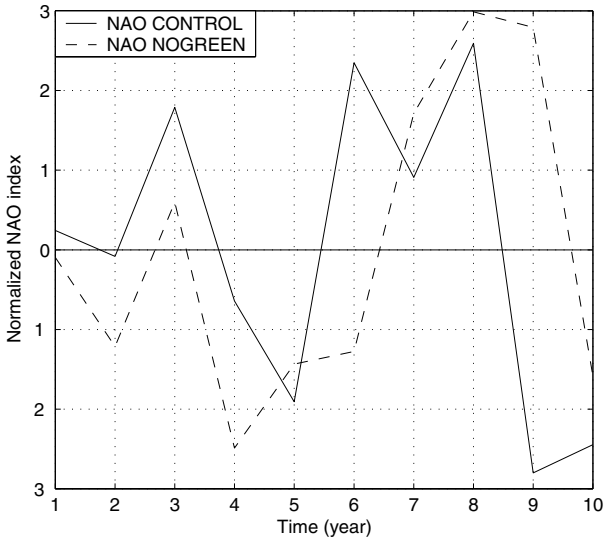

Fig. 9. The normalized winter NAO index in the CONTROL simulation (solid) and the NOGREEN simulation (dashed).

polar region has a rounder shape in the NOGREEN simulation than in the CONTROL simulation where Greenland's impact is found, giving an elongated shape. In other areas there is not a great difference between the simulations.

4. Discussion

The experimental set-up in the present study is simple, the only difference between the two simulations being that the orography of Greenland is removed from the boundary conditions of the NOGREEN simulation. The horizontal extent of Greenland is the same as before, the surface is still defined as a glacier throughout the whole simulation and consequently the albedo is unchanged. It is therefore mainly the impact of Greenland as a large mountain that is isolated. The simulation time is 10 yr, which in the NOGREEN simulation gives the model ample time to form a pseudo-climate, based on a low flat ice-covered island, instead of the Greenland mountain. The results in the present paper should be studied in the light of the GCM applied, the CCM3, as it is possible that some of the results can partly be dependent on the model. The regional biases in the model should

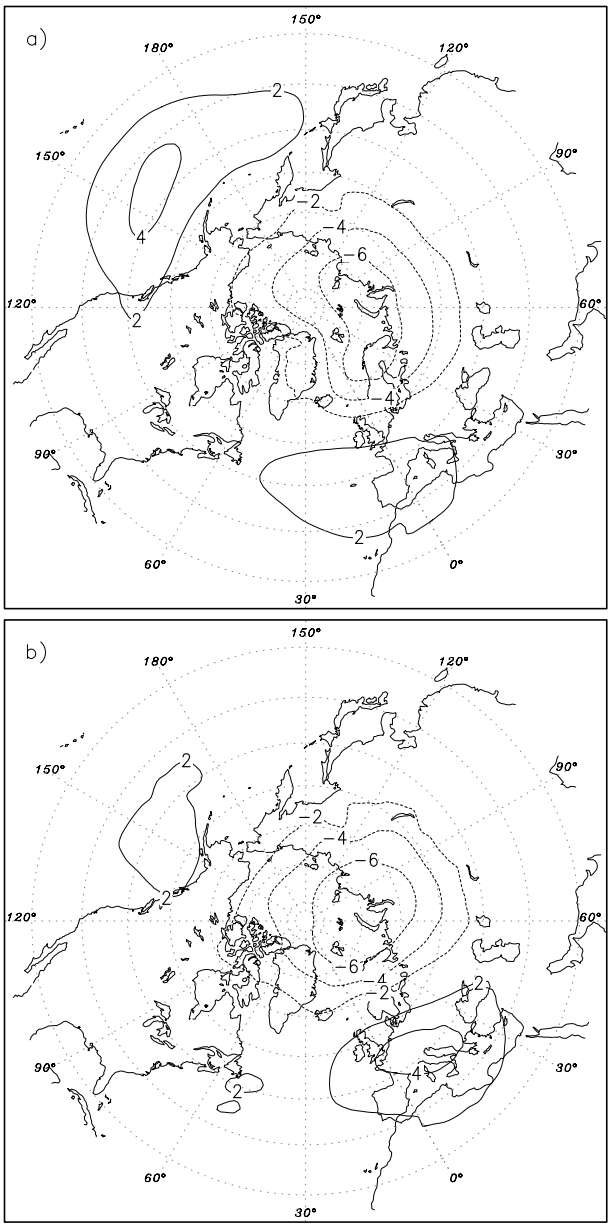

Fig. 10. Leading EOF 1 of the winter mean sea level pressure over the Northern Hemisphere (20°–90°) in (a) the CONTROL simulation and (b) the NOGREEN simulation. The EOF 1 explains 64% of the total variance in (a) and 60% in (b). The patterns are expressed in terms of amplitude (hPa). The contour interval is 2 hPa and the zero contour is suppressed.

be of the same scale in both simulations and thus the difference between the simulations should reflect the impact of Greenland.

Figure 5b shows that there is considerable difference in the 500-hPa geopotential height between the NOGREEN simulation and the CONTROL simulation. The 500-hPa geopotential height difference can have two origins: a difference at the 1000-hPa level or a difference in the geopotential thickness between 1000 and 500 hPa. A comparison of Figures 4b, 5b and 6 shows the following. The slightly lower geopotential height over southern North America and the North Atlantic as well as the higher 500 hPa over central North America and the North Atlantic south of 60°N are caused by changes in the thickness. The increase in the 500-hPa level east of Greenland when the mountain is present is due to the higher sea level pressure while the lower 500-hPa level over Alaska, northern Canada and northern Europe seems to be due to the combined effects of a change at sea level and also in the thickness.

The impact of Greenland seems mainly to be a mechanical blocking or a damming of cold air. On the west side of Greenland, the air mass is cooled down by radiative heat loss during the polar winter over the cold land masses and the sea ice. The mountain acts as a barrier, making it more difficult for the cold air to spread out or to be advected by passing cyclones and thus contributes to colder air masses over northern Canada and Alaska. This cooler air causes a reduction in the 1000–500 hPa geopotential thickness in the area and thus a reduction of the 500-hPa ridge off the western coast of North America. Furthermore, the cold air mass over the Canadian Arctic increases the baroclinicity over North America, resulting in a larger cyclone activity and thus lower sea level pressure in the area. Another possible point of view would be that Greenland causes a difference in the large-scale flow by its impact on the 500-hPa polar vortex which is confined to the west of Greenland but extends farther east in the NOGREEN simulation.

The sea level pressure east of Greenland is higher when the mountain is present. A possible reason for this higher pressure is that Greenland, due to its barrier effect, weakens the flow of cold air from the north and west toward cyclones east of Greenland and consequently weakens the baroclinicity, hence reducing the cyclone strength. This effect was suggested by Kristjánsson and McInnes (1999). A second reason could be that the low-level flow east of northern Greenland, which is on average easterly, piles up air mass at the foot of the mountain in an orographic blocking causing higher pressure. A third possible explanation could be that the high sea level pressure centre, which is often found over Greenland, affects the sea level pressure east of Greenland by increasing northerly cold winds east of Greenland and thus displacing the cyclone tracks southward, see Fig. 7b.

The difference in precipitation rate is compatible with the difference in the storm track structure. The large difference in precipitation rate at the southeastern coast of Greenland is probably at least partly due to the absence of direct orographic lifting when Greenland is flat, but may also be related to the deformation of cyclones passing between Iceland and Greenland (Kristjánsson and McInnes, 1999). Also, the reduction in storm activity over large areas of the North Atlantic in the presence of Greenland results in reduced precipitation.

The difference in the NAO indices between the simulations varies during the simulation time and it is difficult to say whether the two NAO indices show a significant difference. The

differences between the leading EOFs are also difficult to interpret as a significant change in the flow.

The results presented here are mainly on a large scale and the comparison of various fields shows that Greenland seems to have a significant impact on the large-scale flow in the Northern Hemisphere. However, the impact on the Icelandic low is not clear. Due to the complexity of the impact, e.g. mechanical blocking or damming of cold air to the west of the mountain and possible orographic blocking at the northeastern coast, it is not possible to conclude anything about Greenland's impact on the Icelandic low in the present study. This is an interesting research topic that will need more investigations.

5. Summary and conclusions

The present investigation consists of two simulations with the CCM3 applying fine resolution. Although some regional biases known to exist in the model are found, the model simulates the atmospheric circulation reasonably well. The CONTROL simulation is therefore regarded as an approximation to the atmospheric circulation, the NOGREEN simulation to the circulation in Greenland's absence and the difference field as Greenland's impact on the Northern Hemispheric circulation.

The present study shows that Greenland has a significant impact on the general circulation of the Northern Hemispheric extratropics, at both lower and mid-tropospheric levels. Due to the presence of Greenland, the storm tracks are shifted southward over the North Atlantic and thus the mountain contributes to less precipitation at the western coast of Norway and over the North Atlantic. Greenland has a damming effect on the air mass on its west side, which is cooled down by radiative heat loss during the polar winter, leading to less geopotential thickness in the area and thus less 500-hPa geopotential height than in the simulation without Greenland. The cold air also causes increased baroclinicity over North America leading to an increase in cyclone activity. On the east side of Greenland, the mountain causes higher sea level pressure which is associated with increased geopotential height at the 500-hPa level.

The study demonstrates that Greenland's impact on the general circulation is fundamentally different from the impact of the Rocky Mountains and the Tibetan Plateau. Unlike the case of the classic Rossby wave where westerlies impinge on a major mountain range and a trough is created downstream of the mountain, Greenland's impact seems mainly to be a perturbation of the flow on the upstream side of the mountain generated by damming of cold low-level air masses.

6. Acknowledgments

This research is partly financed by the Research Council of Norway (grant 133634/432). This work has received support from The Research Council of Norway (Programme for Supercomputing) through a grant of computing time. We thank James Hack and Philip Rasch at NCAR for suggestions regarding the tuning at T106 resolution and Matthias Münnich for help with the EOF analysis.

References

Blackmon, M. L. 1976. A climatological spectral study of the 500 mb geopotential height of the Northern Hemisphere. *J. Atmos. Sci.* **33**, 1607–1623.

Bromwich, D. H., Du, Y. and Hines, K. M. 1996. Wintertime surface winds over the Greenland ice sheet. *Mon. Wea. Rev.* **124**, 1941–1947.

Bromwich, D. H., Cassano, J. J., Klein, T., Heinemann, G., Hines, K. M., Steffen, K. and Box, J. E. 2001. Mesoscale modeling of katabatic winds over Greenland with the Polar MM5. *Mon. Wea. Rev.* **129**, 2290–2309.

Chang, E. K. M., Lee, S. and Swanson, K. L. 2002. Storm track dynamics. *J. Climate* **15**, 2163–2183.

Chen, Q.-S., Bromwich, D. H. and Bai, L. 1997. Precipitation over Greenland retrieved by a dynamic method and its relation to cyclonic activity. *J. Climate* **10**, 839–870.

Denby, B., Greuell, W. and Oerlemans, J. 2002. Simulating the Greenland atmospheric boundary layer. Part II: Energy balance and climate sensitivity. *Tellus* **54A**, 529–541.

Doyle, J. D. and Shapiro, M. A. 1999. Flow response to large-scale topography: the Greenland tip jet. *Tellus* **51A**, 728–748.

Hack, J. J., Kiehl, J. T. and Hurrel, J. W. 1998. The hydrologic and thermodynamic characteristics of the NCAR CCM3. *J. Climate* **11**, 1179–1206.

Heinemann, G., 1999. The KABEG'97 field experiment: An aircraft-based study of katabatic wind dynamics over the Greenland ice sheet. *Boundary-Layer Meteorol.* **93**, 75–116.

Heinemann, G. and Klein, T. 2002a. Interaction of katabatic winds and mesocyclones near the eastern coast of Greenland. *Meteorol. Appl.* **9**, 407–422.

Heinemann, G. and Klein, T. 2002b. Modelling and observations of the katabatic flow dynamics over Greenland. *Tellus* **54A**, 542–554.

Held, I. M. 1983. Stationary and quasi-stationary eddies in the extratropical troposphere: theory. In: *Large-Scale Dynamical Processes in the Atmosphere* (eds. B. J. Hoskins and R. P. Pearce). Academic Press, London, 127–168.

Hurrell, J. W., Hack, J. J., Boville, B. A., Williamson, D. L. and Kiehl, J. T. 1998. The dynamical simulation of the NCAR Community Climate Model version 3 (CCM3). *J. Climate* **11**, 1207–1236.

Hurrell, J. W., Kushnir, Y., Ottersen, G. and Visbeck, M., eds. 2003. *The North Atlantic Oscillation: Climate Significance and Environmental Impact, Vol. 134 of Geophysical Monograph Series*. American Geophysical Union, Washington, D.C., 279.

Kalnay, E., Kanamitsu, M., Kistler, R., Collins, W., Deaven, D., Gandin, L., Iredell, M., Saha, S., White, G., Woollen, J., Zhu, Y., Leetmaa, A., Reynolds, B., Chelliah, M., Ebisuzaki, W., Higgins, W., Janowiak, J., Mo, K., Ropelewski, C., Wang, J., Jenne, R. and Joseph, D. 1996. The NCEP/NCAR 40-year reanalysis project. *Bull. Am. Meteorol. Soc.*, **77**, 437–471.

Kiehl, J. T., Hack, J. J., Bonan, G. B., Boville, B. A., Briegleb, B. P., Williamson, D. L. and Rasch, P. J. 1996. *Description of the NCAR Community Climate Model (CCM3)*. Technical note, NCAR, Boulder, CO.

Kiehl, J. T., Hack, J. J., Bonan, G. B., Boville, B. A., Williamson, G. L. and Rasch, P. J. 1998. The National Center for Atmospheric Research Community Climate Model: CCM3. *J. Climate* **11**, 1131–1149.

Klein, T., Heinemann, G., Bromwich, D. H., Cassano, J. J. and Hines, K. M. 2001. Mesoscale modeling of katabatic winds over Greenland and comparisons with AWS and aircraft data. *Meteorol. Atmos. Phys.* **78**, 115–132.

Kristjánsson, J. E. and McInnes, H. 1999. The impact of Greenland on cyclone evolution in the North Atlantic. *Q. J. R. Meteorol. Soc.* **125**, 2819–2834.

Magnusdottir, G. 2001. The modeled response of the mean winter circulation to zonally averaged SST trends. *J. Climate* **14**, 4166–4190.

McConnel, J. R., Mosley-Thompson, E., Bromwich, D. H., Bales R. C. and Kyne, J. D. 2000. Interannual variation of snow accumulation on the Greenland ice sheet (1985–1996). *J. Geophys. Res.* **105**, 4039–4046.

Ólafsson, H., 1998. Different prediction of two NWP models of the surface pressure NE of Iceland. *Meteorol. Appl.* **5**, 253–261.

Petersen, G. N., Ólafsson, H. and Kristjánsson, J. E. 2003. Flow in the lee of idealized mountains and Greenland. *J. Atmos. Sci.* **60**, 2183–2195.

Putnins, P. 1970. *World Survey of Climatology: Climate of the Polar Regions* Volume 14. Chapter 2: The Climate of Greenland. Elsevier, Amsterdam, 3–128.

Rossow, W. B. and Schiffer, R. A. 1999. Advances in understanding clouds from ISCCP. *Bull. Am. Meteorol. Soc*., **80**, 2261–2287.

Schwierz, C. B. 2001. *Interaction of Greenland-scale orography and extratropical synoptic-scale flow*. PhD Thesis. Swiss Federal Institute of Technology, Zürich, Switzerland.

Williamson, D. L., Kiehl, J. T. and Hack, J. J. 1995. Climate sensitivity of the NCAR Community Climate Model (CCM2) to horizontal resolution. *Climate Dyn.* **11**, 377–397.

Xie, P. and Arkin, P. A. 1996. Analysis of global monthly precipitation using gauge observations, satellite estimates, and numerical model predictions. *J. Climate*, **9**, 840–858.